Electronic Supplementary Information

# Tunable Rectifications in Nanofluidic Diodes by Ion Selectivity of Charged Polystyrene Opals for Osmotic Energy Conversion

*Tianliang Xiao, Jing Ma, Zhaoyue Liu*, Bingxin Lu, Jiaqiao Jiang, Xiaoyan Nie, Rifeng Luo, Jiao Jin, Qingqing Liu, Wenping Li* and Jin Zhai**

**Content:**

## 1. FT-IR spectra of polystyrene spheres modified with carboxylic (COOH-spheres) and amino groups ($NH_2$-spheres).

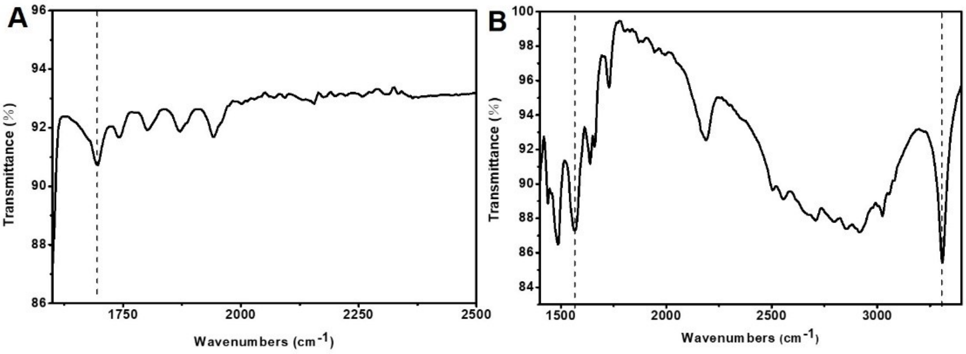

**Figure S1.** FT-IR spectra of COOH-spheres (A) and $NH_2$-spheres (B).

In FT-IR spectra of COOH-spheres (Figure S1A), the peak at 1696 $cm^{-1}$ belongs to C=O stretching vibration.[1] The peaks at 1740, 1802, 1871 and 1943 $cm^{-1}$ belong to C-H out-of-plane bending overtone, which were from benzene ring.[2] In FT-IR spectra of $NH_2$-spheres (Figure S1B), the peaks at 3308 and 1557 $cm^{-1}$ belong to N-H stretching and in-plane bending vibration.[3] The peak at 1490 $cm^{-1}$ belongs to the C-C stretching vibration.[3] The peaks at 1728, 1804, 1870 and 1950 $cm^{-1}$ belong to C-H out-of-plane bending overtone, which were from the benzene ring.[2] The peak at 2189 $cm^{-1}$ belongs to C-N stretching vibration.[4]

## 2. XPS spectra of polystyrene microspheres modified with carboxylic and amino groups.

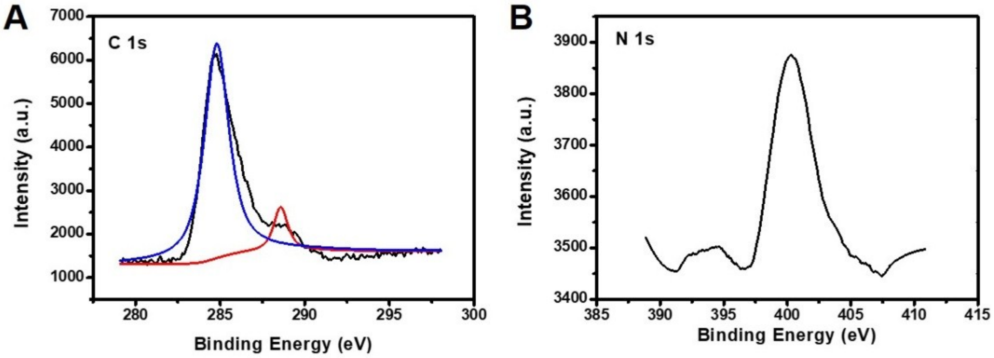

**Figure S2.** XPS spectra of polystyrene microspheres modified with carboxylic (A) and amino groups (B).

### 3. Characterizations of the opals formed by COOH-spheres (COOH-opals) with an average sphere diameter of 208 nm.

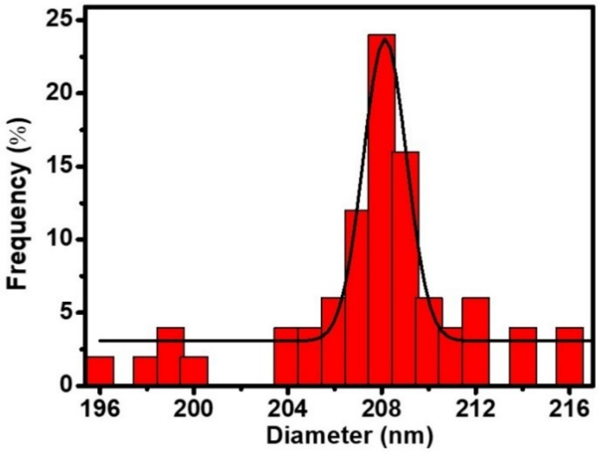

**Figure S3.** The size distribution histograms and the Gaussian distributions of COOH-spheres with an average diameter of 208 nm.

The size distribution of polystyrene spheres was based the diameter of 50 spheres determined from magnified top-viewed SEM image. The distribution was shown as a histogram, which was fitted by a Gaussian distribution. The average diameter of polystyrene spheres was obtained from the peak value of the Gaussian distribution.

## 4. Schematic diagram for the definition of the nano-gaps for ion transport and the size distribution of nano-gaps in opals with an average sphere diameter of 208 nm.

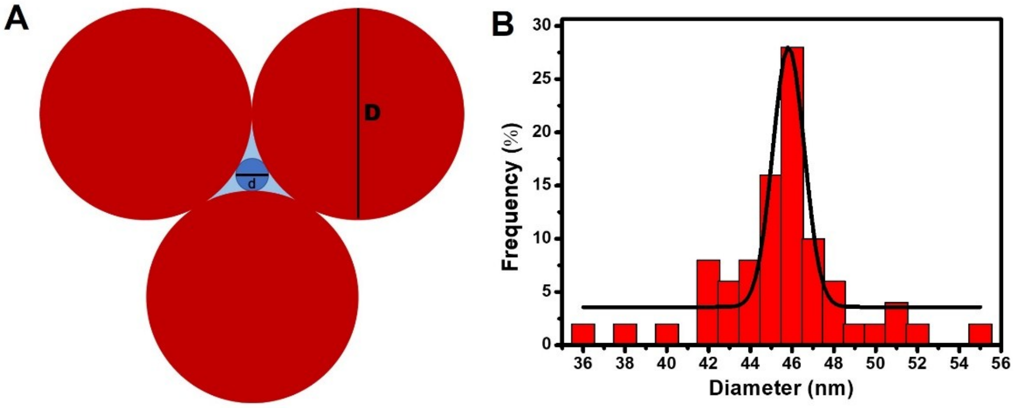

**Figure S4.** (A) Schematic diagram for the definition of the nano-gaps formed the spheres. The diameter (*d*) of the nano-gaps formed by three adjacent spheres with a diameter of *D* was defined to be the channel size for ion transport in opals. The value of *d* was mathematically calculated to be $\frac{\left(2\sqrt{3}-3\right)D}{3}$. (B) The diameter of the nano-gaps formed by the COOH-spheres in the opals with an average sphere diameter of 208 nm, which was determined from SEM images.

## 5. Characterizations of an AAO membrane.

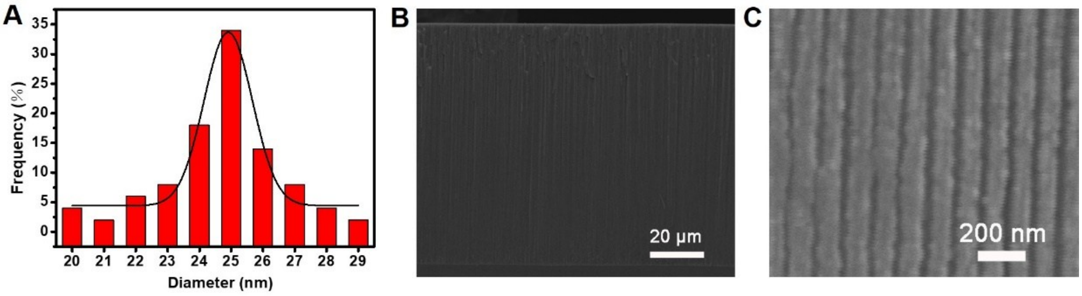

**Figure S5.** Characterizations of an AAO membrane. (A) The size distribution histograms and the Gaussian distributions for the nanopores of AAO determined from SEM images. (B) The thickness of AAO membrane was ~88 μm. (C) Magnified image of the cylindrical nanochannel of AAO membrane.

## 6. The magnified cross-sectional SEM image of an opal layer on an anodized aluminum oxide support.

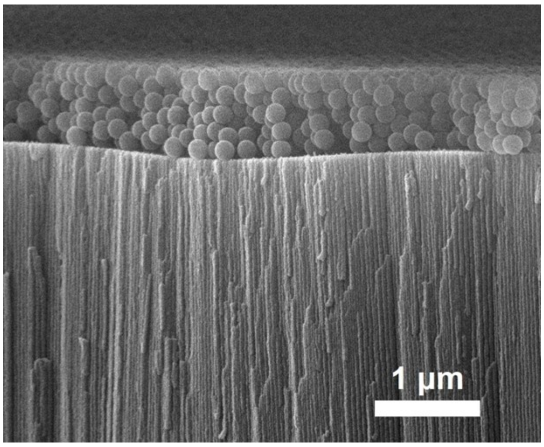

**Figure S6.** The magnified cross-sectional SEM image of an opal layer on an anodized aluminum oxide support. The opal demonstrated a multilayer structure.

### 7. Schematic setup for the measurement of ion current.

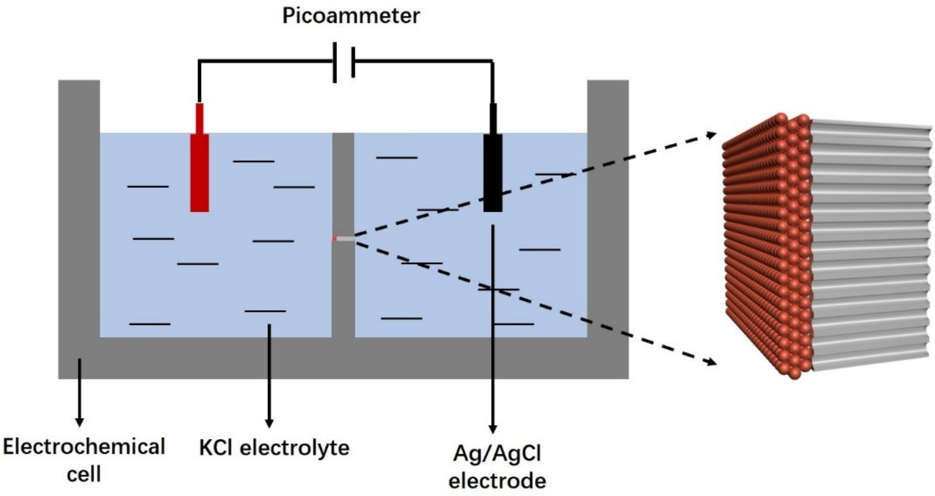

**Figure S7.** Schematic setup for the measurement of ion current-voltage (*I*-*V*) curves. The diode membrane was mounted between the two chambers of an electrochemical cell. 1 mM of KCl aqueous solution with a pH value of 5.0 was used as the electrolyte. A pair of Ag/AgCl electrodes was used to apply the transmembrane voltage. The opal side was fixed as an anode.

## 8. Theoretical model of COOH-opals/AAO and $NH_2$-opals/AAO.

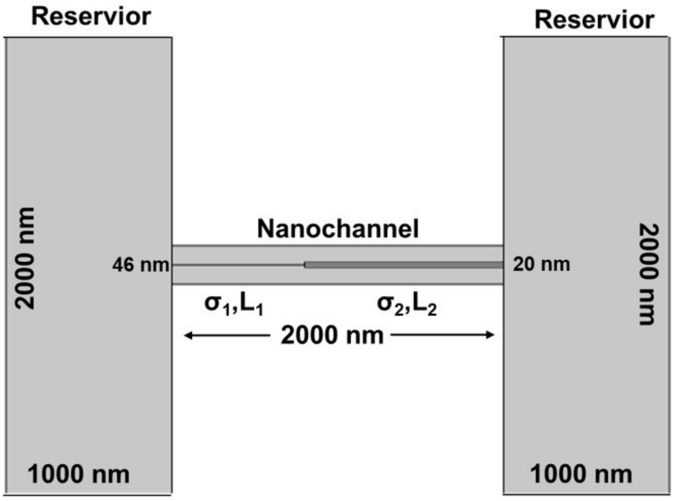

**Figure S8.** Theoretical model of COOH-opals/AAO and $NH_2$-opals/AAO.

To simplify the calculation, diodes of 208-nm-COOH-opals/AAO and 176-nm-$NH_2$-opals/AAO were theoretically modeled as double-layer nanochannels consisting of 46 nm-width opal cylindrical nanochannels coated on 20 nm-width AAO cylindrical nanochannel. The total length of the nanochannel was set to be 2000 nm, which contained opal segment of 800 nm and AAO segment of 1200 nm.

The ion transport properties of above diodes were quantitatively calculated using "Electrostatics" and "Transport of Diluted Species" modules in COMSOL Multiphysics 5.4. [5] $\sigma_1$ and $L_1$ are the surface charge density and the length of opal segment. $\sigma_2$ and $L_2$ are those of AAO side.

The calcualtion was carried out based on the Poisson, Nernst–Planck equations and the steady state continuous equations.[6,7]

$$\nabla^2\phi =- \frac{F^2}{\varepsilon}\sum z_i c_i$$

$$J_i =- D_i \ \left(\nabla c_i + \frac{z_i F c_i}{RT}\nabla\phi\right)$$

$$\nabla J_i = 0$$

In these equations, $\varphi$, $z_i$, $c_i$, $J_i$ and $D_i$ denote electrical potential, the charge number, the ionic concentration, the ionic flux and the diffusion coefficient of each species $i$, respectively. The boundary conditions of the nanochannel are as follows:

$$\vec{n} \cdot \nabla\phi = -\frac{\sigma}{\varepsilon}$$

$$\vec{n} \cdot J_i = 0$$

Where $\vec{n}$ and $\sigma$ represent the unit normal vector and the surface charge density, respectively.

The ionic current of species *i* can be calculated by integrating the ionic flux along the cross section of the nanochannel:

$$I_i = \int_s J_i ds = -\int_s D_i(\nabla c_i + \frac{z_i F c_i}{RT}\nabla\phi) ds$$

The surface charge densities of COOH-opals, $NH_2$-opals and AAO were set as -10 μC/m$^2$, +10 μC/m$^2$ and +0.5 mC/m$^2$.

## 9. Ion transport property of a blank AAO membrane.

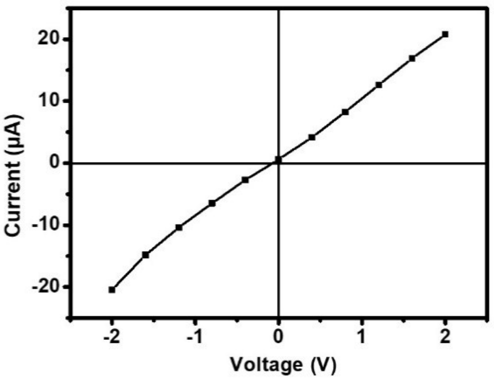

**Figure S9.** *I*-*V* curve of a blank AAO membrane without ion rectification property.

## 10. Characterizations of the COOH-spheres with various sizes.

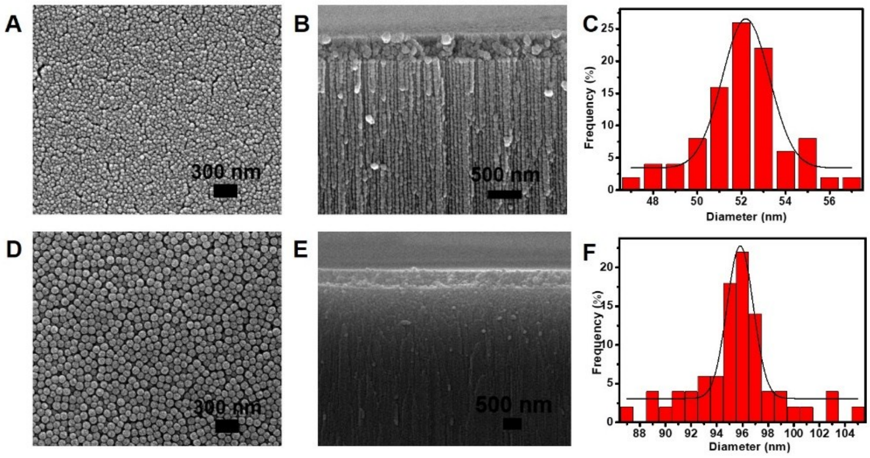

**Figure S10.** Top-viewed, cross-sectional SEM images and size distribution histograms and the Gaussian distributions for the COOH-spheres with diameter of ~52 nm (A, B and C) and ~96 nm (D, E and F).

## 11. Characterizations of $NH_2$-spheres with various sizes.

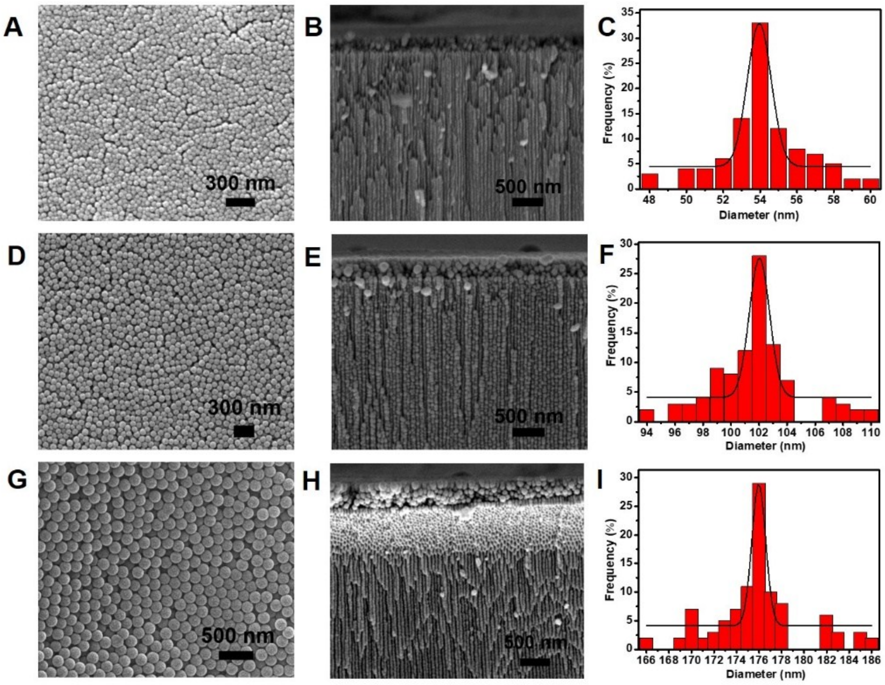

**Figure S11.** Top-viewed, cross-sectional SEM images and size distribution histograms and the Gaussian distributions for the $NH_2$-spheres with an average of diameter of 54 nm (A, B and C), 102 nm (D, E and F) and 176 nm (G, H and I).

## 12. Cross-sectional SEM images of diode-cba, diode-bca and diode-cab.

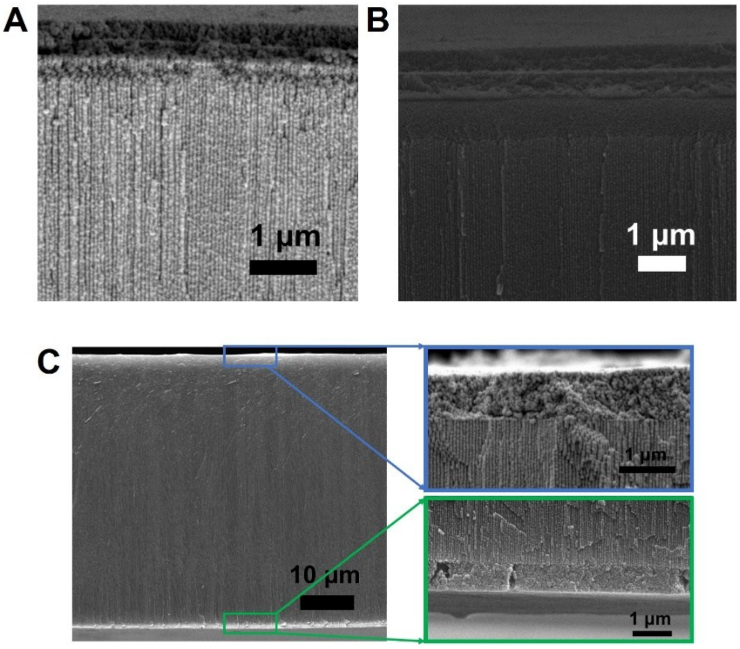

**Figure S12.** Cross-sectional SEM images of diode-cba (A), diode-bca (B) and diode-cab (C). Diode-cba was composed of $NH_2$-opals/COOH-opals/AAO, while diode-bca was composed of COOH-opals/$NH_2$-opals/AAO. Diode-cab showed a sandwiched structure of $NH_2$-opals/AAO/COOH-opals.

## 13. Theoretical model of $NH_2$-opals/COOH-opals/AAO (diode-cba), COOH-opals /$NH_2$-opals/AAO (diode-bca) and $NH_2$-opals/AAO/COOH-opals (diode-cab).

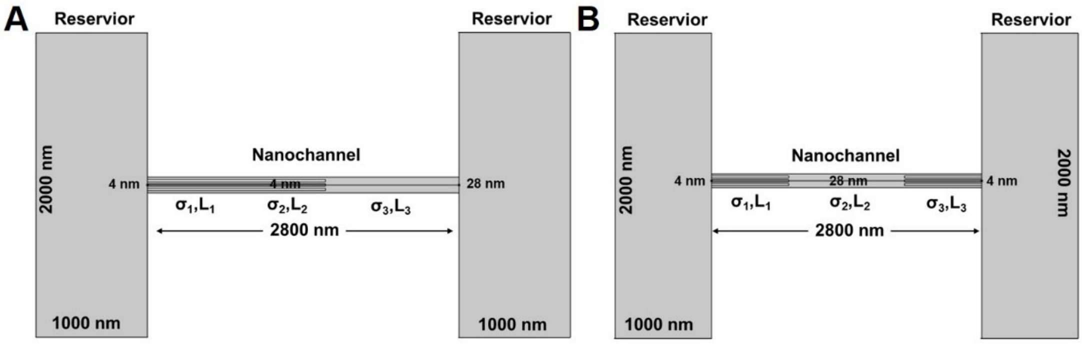

**Figure S13.** Theoretical model of $NH_2$-opals/COOH-opals/AAO (diode-cba), COOH-opals /$NH_2$-opals/AAO (diode-bca) (A) and $NH_2$-opals/AAO/COOH-opals (diode-cab) (B).

To simplify the calculation, diode-cba and diode-bca were theoretically modeled as triple-layer nanochannels consisting of two layers of 4 nm-width opal cylindrical nanochannels coated on a single 28 nm-width AAO cylindrical nanochannel. The total length of the nanochannel was set to be 2800 nm, which contained two opal segments of 800 nm and AAO segment of 1200 nm. Diode-cab was theoretically modeled as sandwiched nanochannels consisting of a single 28 nm-width AAO cylindrical nanochannel sandwiched by two layers of 4 nm-width opal cylindrical nanochannels. The total length of the nanochannel was set to be 2800 nm, which contained AAO segment of 1200 nm and two opal segments of 800 nm.

The surface charge densities of COOH-opals, $NH_2$-opals and AAO were set as -10 $\mu C/m^2$, +10 $\mu C/m^2$ and +0.5 $mC/m^2$.

## 14. Schematic diagram for the device of power generation from osmotic energy and the electrode calibration.

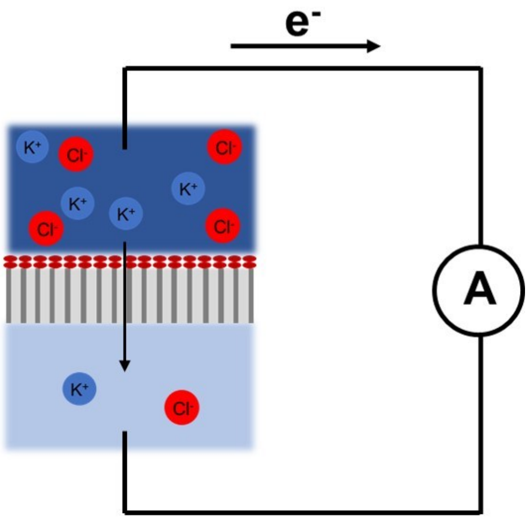

**Figure S14.** Schematic diagram for a device of power generation from osmotic energy.

The measured open-circuit voltage ($E_{\mathrm{mea}}$) consists of two contributions from the redox potential difference of the two Ag/AgCl electrodes ($E_{\mathrm{redox}}$) and the diffusion potential of diode membrane ($E_{\mathrm{diff}}$) as described by the following equation:[8]

$$E_{\mathrm{mea}} = E_{\mathrm{redox}} + E_{\mathrm{diff}}$$

In order to obtain the $E_{\mathrm{redox}}$ value at a concentration gradient, a non-selective silicon micropore with a geometric area of 0.0001 $\mathrm{mm}^2$ was used for ion transport. In this case, $E_{\mathrm{mea}} = E_{\mathrm{redox}}$. Then the value of $E_{\mathrm{diff}}$ contributed by the diode membrane was easily obtained by the following equation:

$$E_{\mathrm{diff}} = E_{\mathrm{mea}} - E_{\mathrm{redox}}$$

## 15. The $V_{oc}$ and $I_{sc}$ of diode-bca, diode-cba, diode-ca and diode-cab under different concentration gradient.

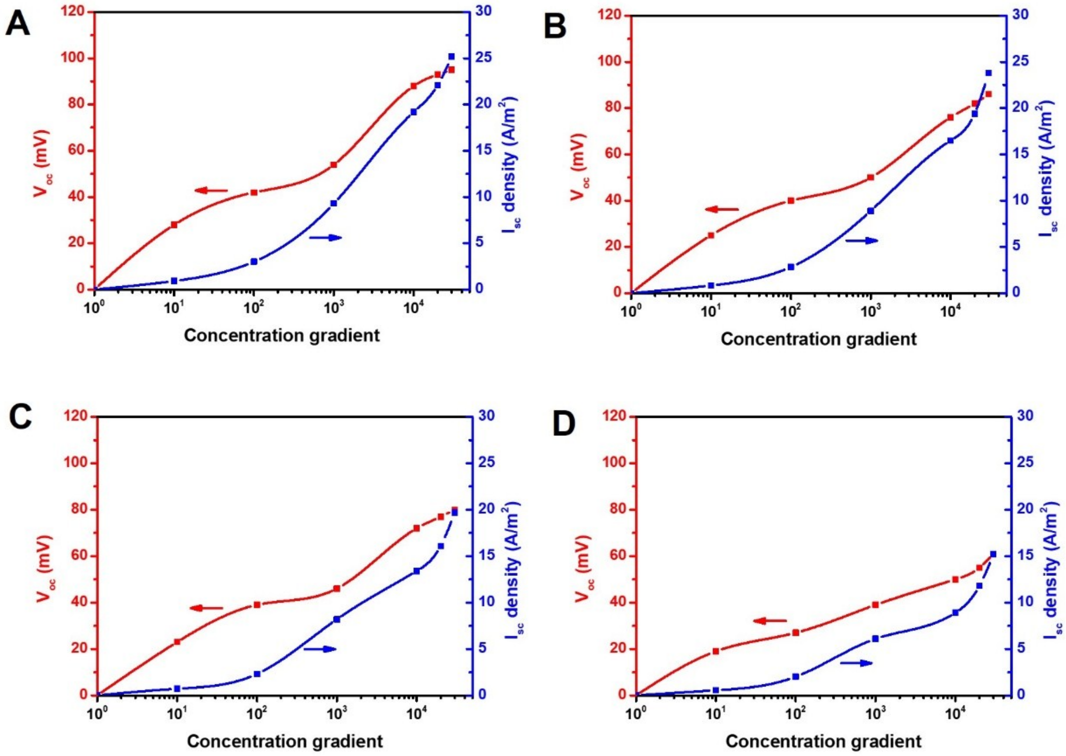

**Figure S15**. The $V_{oc}$ and $I_{sc}$ of diode-bca (A), diode-cba (B), diode-ca (C) and diode-cab (D) under different concentration gradient. Diode-cba: $NH_2$-opals/COOH-opals/AAO; Diode-bca: COOH-opals/$NH_2$-opals/AAO; Diode-cab: $NH_2$-opals/AAO/COOH-opals.

## 16. The measured voltage ($E_{\text{mea}}$), redox potential difference ($E_{\text{redox}}$), and diffusion potential ($E_{\text{diff}}$) of COOH-opals/AAO (diode-ba).

**Table S1.** The measured voltage ($E_{\text{mea}}$), redox potential difference ($E_{\text{redox}}$), and diffusion potential ($E_{\text{diff}}$) of COOH-opals/AAO (diode-ba).

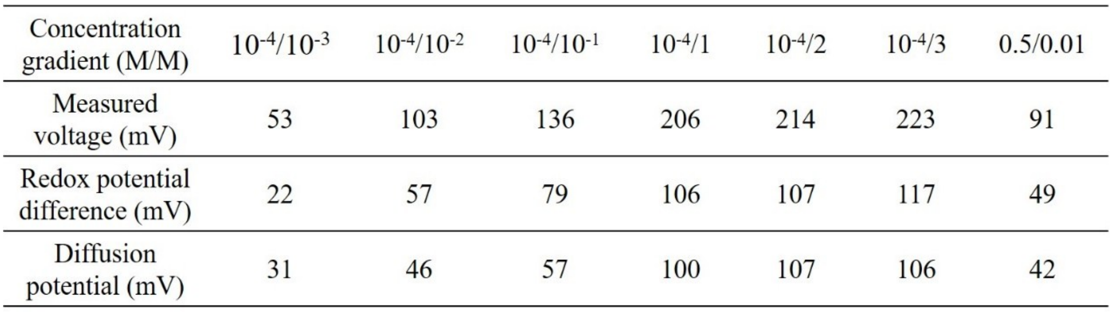

| Concentration gradient (M/M) | $10^{-4}/10^{-3}$ | $10^{-4}/10^{-2}$ | $10^{-4}/10^{-1}$ | $10^{-4}/1$ | $10^{-4}/2$ | $10^{-4}/3$ | 0.5/0.01 |
|---|---|---|---|---|---|---|---|
| Measured voltage (mV) | 53 | 103 | 136 | 206 | 214 | 223 | 91 |
| Redox potential difference (mV) | 22 | 57 | 79 | 106 | 107 | 117 | 49 |
| Diffusion potential (mV) | 31 | 46 | 57 | 100 | 107 | 106 | 42 |

## 17. The output of current and power density of diode-bca, diode-cba, diode-ca and diode-cab under a salinity gradient of $c_H/c_L$ = 0.5 M/0.01 M.

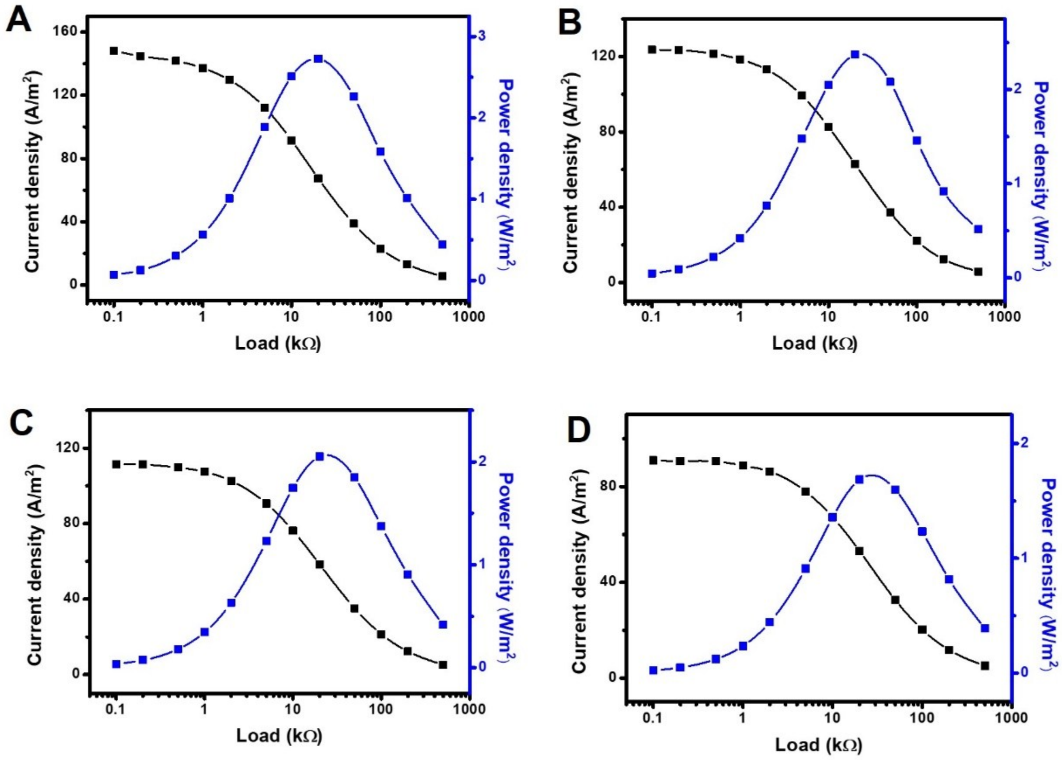

**Figure S16.** The output of current and power density of diode-bca (A), diode-cba (B), diode-ca (C) and diode-cab (D) under a salinity gradient of $c_H/c_L$ = 0.5 M/0.01 M. Diode-cba: $NH_2$-opals/COOH-opals/AAO; Diode-bca: COOH-opals/$NH_2$-opals/AAO; Diode-ca: $NH_2$-opals/AAO; Diode-cab: $NH_2$-opals/AAO/COOH-opals.

## 18. References

[1] V. Lochar and H. Drobna, *Appl. Catal. A-Gen.*, 2004, **269**, 27.

[2] M. M. Nasef, H. Saidi and H. M. Nor, *J. Appl. Polym. Sci.*, 2000, **76**, 220.

[3] N. Sundaraganesan, S. Ilakiamani and B. D. Joshua, Spectroc. *Acta Pt. A-Molec. Biomolec. Spectr.*, 2007, **67**, 287.

[4] M. Sivanantham, R. Kesavamoorthy, T. N. Sairam, K. N. Sabharwal and B. Raj, *J. Polym. Sci., Part B: Polym. Phys.*, 2008, **46**, 710.

[5] Q. Zhang, Z. Zhang, H. Zhou, Z. Xie, L. Wen, Z. Liu, J. Zhai and X. Diao, *Nano Res.,* 2017, **10**, 3715.

[6] I. Vlassiouk, S. Smirnov and Z. Siwy, *ACS Nano,* 2008, **2**, 1589.

[7] H. Daiguji, Y. Oka and K. Shirono, *Nano Lett.,* 2005, **5**, 2274.

[8] D. Kim, C. Duan, Y. Chen and A. Majumdar, *Microfluid. Nanofluid.* 2010, **9**, 1215.